Am J Physiol Regulatory Integrative Comp Physiol
281: R206–R212, 2001.

Dynamic relationship between sympathetic nerve activity and renal blood flow: a frequency domain approach

SARAH-JANE GUILD,[1] PAUL C. AUSTIN,[1] MICHAEL NAVAKATIKYAN,[1]
JOHN V. RINGWOOD,[2] AND SIMON C. MALPAS[1]
[1]*Circulatory Control Laboratory, Departments of Physiology and Electrical and Electronic Engineering, University of Auckland, New Zealand; and* [2]*Department of Electronic Engineering, National University of Ireland, Maynooth, County Kildare, Ireland*

Received 20 November 2000; accepted in final form 27 February 2001

Guild, Sarah-Jane, Paul C. Austin, Michael Navakatikyan, John V. Ringwood, and Simon C. Malpas. Dynamic relationship between sympathetic nerve activity and renal blood flow: a frequency domain approach. *Am J Physiol Regulatory Integrative Comp Physiol* 281: R206–R212, 2001.—Blood pressure displays an oscillation at 0.1 Hz in humans that is well established to be due to oscillations in sympathetic nerve activity (SNA). However, the mechanisms that control the strength or frequency of this oscillation are poorly understood. The aim of the present study was to define the dynamic relationship between SNA and the vasculature. The sympathetic nerves to the kidney were electrically stimulated in six pentobarbital-sodium anesthetized rabbits, and the renal blood flow response was recorded. A pseudo-random binary sequence (PRBS) was applied to the renal nerves, which contains equal spectral power at frequencies in the range of interest (<1 Hz). Transfer function analysis revealed a complex system composed of low-pass filter characteristics but also with regions of constant gain. A model was developed that accounted for this relationship composed of a 2 zero/4 pole transfer function. Although the position of the poles and zeros varied among animals, the model structure was consistent. We also found the time delay between the stimulus and the RBF responses to be consistent among animals (mean 672 ± 22 ms). We propose that the identification of the precise relationship between SNA and renal blood flow (RBF) is a fundamental and necessary step toward understanding the interaction between SNA and other physiological mediators of RBF.

modeling; pseudo-random binary sequence

SYMPATHETIC NERVE ACTIVITY (SNA) has been proposed to play an important role in the regulation of renal blood flow (RBF) (12). Whereas much previous research has focused on how the mean level of SNA regulates the mean level of RBF in response to a range of afferent stimuli (10), there has been little consideration given to fact that SNA is a signal made up of multiple frequency bands, ranging from 10 to 0.1 Hz (9). Surprisingly little is known about how these frequency components impact on the renal vasculature. Mathematical models have been developed to describe the effect blood pressure has on RBF (4–6). These models have proven useful in understanding the dynamics of autoregulation and tubuloglomerular feedback; however, there is a paucity of information on the dynamics of the neural control of RBF. Information on how the various frequencies in SNA regulate RBF is likely to be valuable in understanding the origin of oscillations present in blood pressure (2) and in predicting how diseases or therapeutic treatments that alter SNA could affect the control of RBF and potentially blood pressure.

Previous work by our lab has determined that the renal vasculature appears only able to follow frequencies in SNA below 0.7 Hz, with frequencies above this level producing steady vascular tone (11). The corresponding frequency response characteristics suggested that a first-order model with a time delay could be suitable in describing the neural control of RBF. However, our previous method of activating the renal nerves did not allow determination of model parameters with any degree of accuracy. Identification of such a model structure would allow a starting point for determining the physiological basis for the impact of sympathetic activity on the renal vasculature (i.e., the frequency response) and the interaction with possible mediators of this response, e.g., tubuloglomerular feedback or circulating vasoconstrictive hormones. The aim of this study therefore is to describe in detail the dynamics of neural control over RBF and develop a more complete mathematical model with associated parameters.

METHODS

Experiments were performed on New Zealand White rabbits (n = 6, mean weight 2.9 ± 0.1 kg) and were approved by the University of Auckland Animal Ethics Committee. Animals were allowed food and water ad libitum until the experimental procedures began.

Surgical procedures. Induction of anesthesia was by intravenous administration of pentobarbital sodium (90–150 mg Nembutal; Virbac Laboratories, Auckland, New Zealand) and was immediately followed by endotracheal intubation

Address for reprint requests and other correspondence: S. C. Malpas, Circulatory Control Laboratory, Dept. of Physiology, Univ. of Auckland Medical School, Private Bag 92019, Auckland, New Zealand (E-mail: s.malpas@auckland.ac.nz).

The costs of publication of this article were defrayed in part by the payment of page charges. The article must therefore be hereby marked "*advertisement*" in accordance with 18 U.S.C. Section 1734 solely to indicate this fact.

and artificial respiration. Anesthesia was maintained throughout the surgery and experiment by pentobarbital infusion (30–50 mg/h).

During surgery 154 mmol/l NaCl solution was infused intravenously at a rate of 0.18 $ml \cdot kg^{-1} \cdot min^{-1}$ to replace fluid losses. A heated blanket was used throughout the surgery and experiment to maintain body temperature at ~36°C. A catheter was inserted into the central ear artery for monitoring arterial pressure. The left kidney was approached via a retroperitoneal incision, and the renal artery and nerves were carefully exposed. A transit time flow probe (type 2SB Transonic Systems, Ithaca, NY) was placed around the renal artery. The kidney was then freed from the peritoneal lining and surrounding fat and placed in a stable cup. The renal nerves were identified using a surgical microscope and placed across a pair of hooked stimulating electrodes. The nerves were then sectioned proximal to the stimulating electrodes. Paraffin oil was applied to the nerves throughout the experiment to prevent dehydration.

Data acquisition. The ear artery catheter was connected to a pressure transducer (Cobe, Arvarda, CO) and the transit-time flow probe was connected to a compatible flowmeter (T106, Transonic Systems). These analog signals were digitized and continuously displayed by the nerve stimulation program, allowing continuous sampling of mean arterial pressure (MAP, mmHg) and renal blood flow (RBF, ml/min). Heart rate (HR, beats/min) was derived from the MAP waveform. During each experiment, data were saved continuously.

Experimental protocol. Electrical stimulation of the renal nerves was produced using purpose-written software in the LabVIEW graphical programming language (National Instruments, Austin, TX) coupled to a LabPC+ data-acquisition board (National Instruments). Initially, it was important to determine a stimulus voltage that gave the maximum decrease in RBF without being supramaximal. This was determined by giving short periods (30 s) of 4-Hz stimuli at various voltages to the renal nerves and recording the RBF response. This voltage was used as the upper limit of voltage for each stimulus sequence. After a 5-min control period, the renal nerves were then stimulated using a pseudo-random binary sequence (PRBS). The PRBS stimulation was composed of a base frequency of 4 Hz (2-ms pulse width) whose amplitude switched between the upper voltage (determined previously) and a low voltage (0.5 V). Every 0.5 s a decision was made to switch between the high voltage and the low voltage or to stay at the current voltage (Fig. 1). This creates a signal with a flat power spectrum across the frequency range of interest (0–1 Hz). This frequency range was chosen because previous work (11) showed that frequencies above ~0.7 Hz have little effect dynamically on RBF. The PRBS stimulus was applied to the nerve for a period of 30 min.

Validation of PRBS. Previously, we used sinusoidal nerve stimulation to determine the frequency response characteristics of the renal vasculature. To validate the PRBS approach in each animal, we also applied sinusoidal stimulation. Details of this form of stimulation have already been published (11); briefly, a base frequency of 4 Hz was applied to the renal nerves where the amplitude of the individual pulses (2-ms pulse width) varied in a sine fashion. The modulated sine stimulation was delivered at the following frequencies applied in a random order: 0.04, 0.08, 0.12, 0.16, 0.2, 0.25, 0.32, 0.4, 0.5, and 0.72 Hz for periods of 7 min with 5-min recovery periods. Spectral analysis

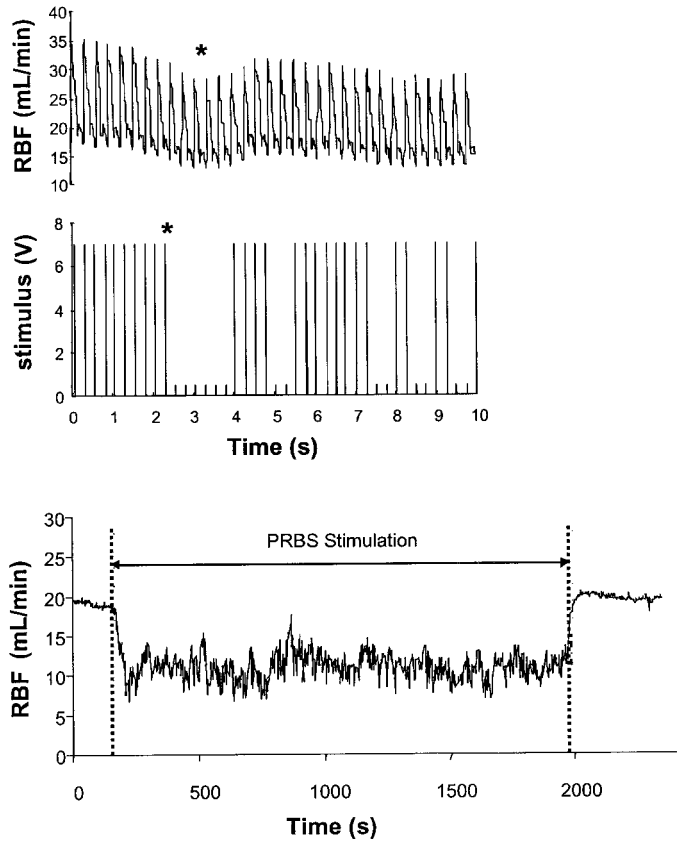

Fig. 1. Response of renal blood flow (RBF) to pseudo-random binary sequence (PRBS) stimulation for 10 s (*top*) and mean RBF response of the full 30 min (*bottom*). Note the time delay between the change in stimulus voltage and the RBF response (*).

was used to determine the amplitude of the induced oscillations in RBF, and this amplitude was compared with that obtained for the PRBS transfer function.

Data analysis. The 500-Hz sampled data of RBF and the stimulus were reduced to 2-Hz sampled data using the decimate function in the Signal Processing Toolbox of MatLab (The Mathworks, Natick, MA), which applied an eighth-order Chebychev filter to each signal in the forward and reverse directions to remove any phase distortion introduced by filtering before the signals were resampled at the new sampling rate. The 2-Hz sampled data then underwent a fast Fourier transform to determine the spectral components of each signal. The resulting frequency resolution was 0.0008 Hz. The transfer function between the stimulus and the RBF response was calculated by dividing the cross spectrum of the stimulus and RBF by the autospectrum of the stimulus using MatLab. The magnitude response was plotted as decibels (20 $\log_{10}$ of the gain). Phase plots are shown such that RBF is always after the stimulus, and the inverse relationship between RBF and stimulus was accounted for by removing 180 degrees from the phase. To give an indication of how well the two signals were coupled, the coherence, C_{xy}, between stimulus and RBF was calculated. This was done using MatLab and the relationship in *Eq. 1*, where P_{xy} is the cross spectrum and P_{xx} and P_{yy} are the power spectra of *signals x* and *y*, respectively. Nonoverlapping sections of 256 data points were used in the coherence calculations. Data are repre-

sented as means ± SE. *Equation 1* is the calculation of coherence between two signals, x and y.

$$C_{xy} = \frac{|P_{xy}(f)|^2}{P_{xx}(f)P_{yy}(f)} \quad (1)$$

RESULTS

Effects of PRBS stimulation. The stimulation of the renal nerves with the PRBS sequence caused a mean decrease in RBF of 12 ± 2 ml/min (control RBF 33 ± 4 ml/min, $n = 6$), whereas MAP and HR remained constant (69 ± 3 mmHg and 247 ± 15 beats/min, respectively). This mean reduction in RBF was stable throughout the entire 30-min period of stimulation (Fig. 1). The reduction in RBF was associated with increased variability due to the stimulus. When the RBF response to the stimulus was examined over shorter time scales, there was evidence of a time delay between a change in the stimulus level and a change in renal blood flow (2).

Calculation of the magnitude response between the stimulus and RBF indicated a decreasing ability for the renal vasculature to follow the stimulus as the frequency of the stimulus increased (Fig. 2). For example, the effect of stimulus at 0.6 Hz was ~40% of the effect of the same stimulus intensity at 0.2 Hz in RBF. Stimuli between 0.01 and 0.2 Hz appeared to result in the same size responses in RBF. In several animals there was evidence of increased gain in between 0.1 and 0.2 Hz causing the appearance of a "bump" in the magnitude response (Fig. 3*B*). Subsequently, <0.01 Hz there was a small range of frequencies that caused an even larger response in RBF. Overall this gain response suggested a 2 zero/4 pole system. This was derived from the asymptotes of the gain plot, the gradients of which must be multiples (positive or negative) of 20 dB/decade. The first change in slope of −20 dB/decade indicates the presence of a low-frequency pole. This is followed by a 20 dB/decade positive change in slope, suggesting the presence of a zero. The effect of this positive change (zero) was to counteract the earlier pole and produce a flat gain response between 0.01 and 0.2 Hz. The bump in some animals required the presence of a second zero at this point to cause the increase in gain. The third change in slope of −40 dB/decade suggests the presence of a double pole. The fourth pole was required to counteract the effect of the second zero, either at the same position as the second zero to produce the flat region of gain or at the position of the double pole to create the 40 dB/decade slope after the bump. The combination of the poles and zeros in a transfer function gave a set of seven parameters that were defined (*Eq. 2*), where K is the DC gain, and the five ω parameters are the positions of the poles and zeros, with ζ representing the damping factor for the double pole at ω_5. *Equation 2* is the 2 zero/4 pole transfer function showing the fitted parameters.

$$G(s) = \frac{K\left(1+\frac{s}{\omega_1}\right)\left(1+\frac{s}{\omega_2}\right)e^{-s\tau}}{\left(1+\frac{s}{\omega_3}\right)\left(1+\frac{s}{\omega_4}\right)\left[1+2\zeta\frac{s}{\omega_5}+\left(\frac{s}{\omega_5}\right)^2\right]} \quad (2)$$

The general linear shape of the phase plot indicates the presence of a pure time delay (1). At the lower frequencies (<0.2 Hz) there is a deviation from the linear relationship, representing the presence of a dynamic lag that is dependent on the frequency of stimulation. The pure time delay was the eighth parameter (τ) to be fitted to the data from each rabbit.

Each of the eight parameters from *Eq. 2* was determined to minimize the difference between the transfer function information calculated from the experimental data and that defined by the model parameters. A cost function was defined as

$$J = \sum_i \left[(|G_i| - |\hat{G}_i|)^2 + \frac{\max(|G_i|)}{\max(\angle G_i)} (\angle G_i - \angle \hat{G}_i)^2 \right]$$

The weighting, $\max(|G_i|)/\max(<G_i)$, was used to increase the size of the error in the phase information to counter the weighting toward the magnitude information caused by the large size of the numbers involved. Without this weighting on the phase error, the phase information had little effect on the resulting parameter values that were largely determined by the magnitude response. The optimization was done using "fminsearch," a MatLab routine that uses the simplex search method to find the minimum of the given cost function. The mean pure time delay (τ) was found to be 0.67 ± 0.02 s ($n = 6$). Although between individual rabbits there was a relatively wide spread of values for each model parameter (Table 1), producing variation in the

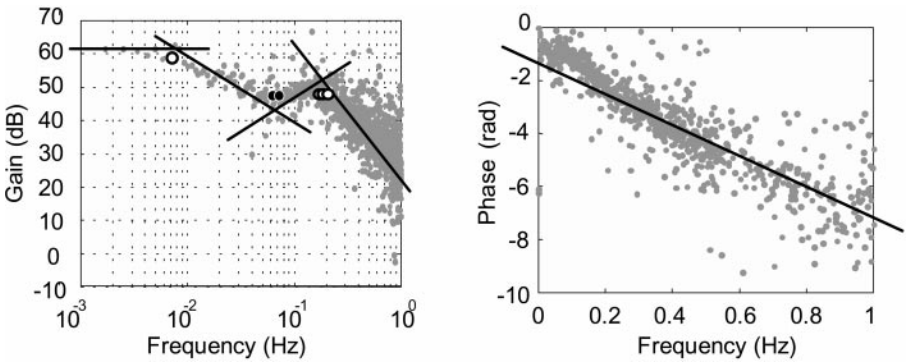

Fig. 2. Magnitude and phase response data for a single rabbit (gray dots), with lines drawn to suggest the appropriate model structure (2 zeros/4 poles). ○, Position of the poles; ●, the zeros. A pure time delay was indicated by the linear relationship to frequency in the phase data.

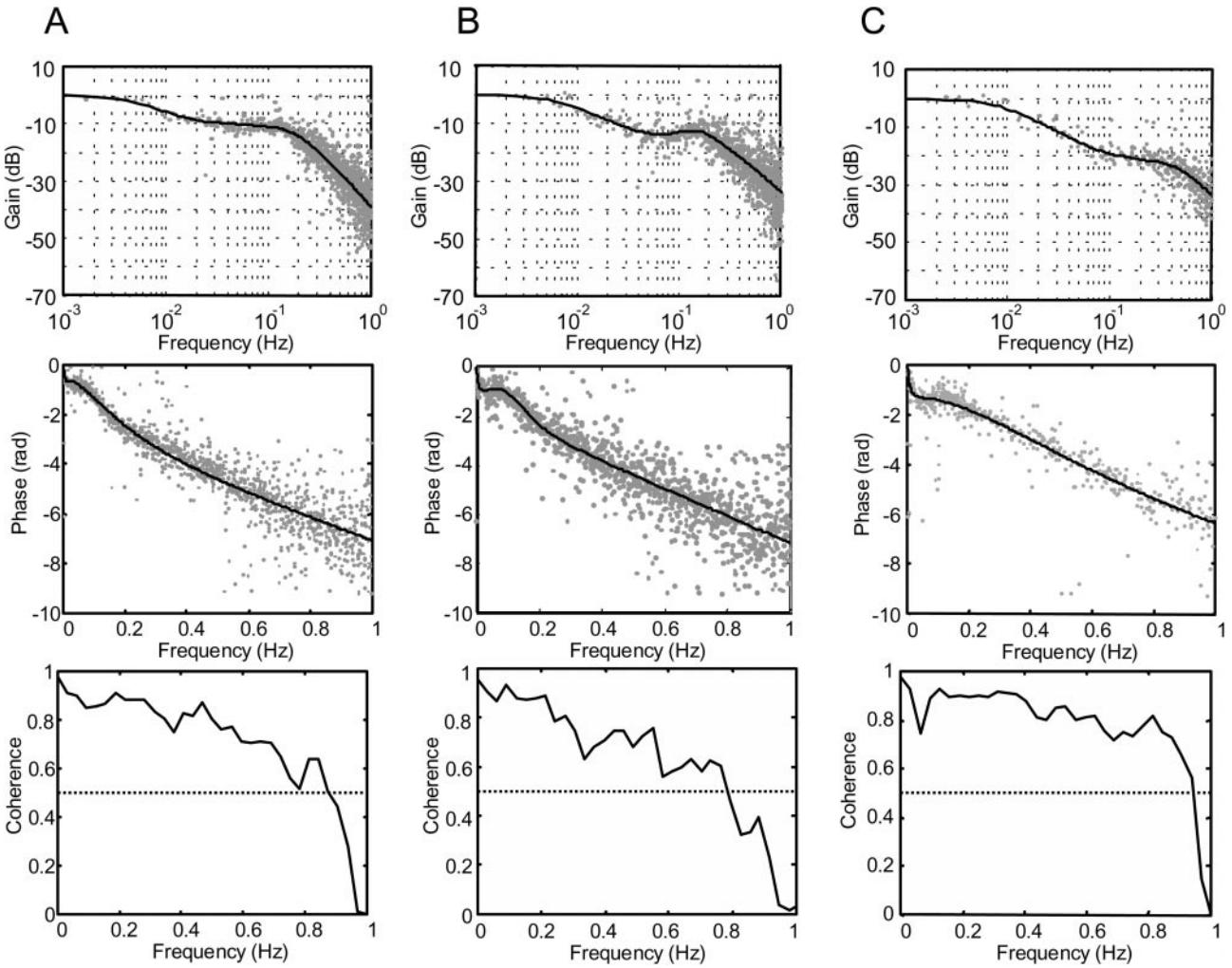

Fig. 3. Transfer functions between electrical stimulation and the RBF response for 3 rabbits (gray dots). Solid line indicates the derived model. For ease of comparison among rabbits, the gain plots show the gain normalized with respect to the DC gain (K) from the models. Note the high degree of coherence up to 0.8 Hz (the dotted line on the coherence plot indicates a coherence value of 0.5). Although the model structure was the same among animals, there were differences in the position of the poles and zeros, e.g., the curve for *rabbit C* was shifted to the right.

position of the poles and zero, importantly the same model structure was found to be appropriate for all rabbits (Fig. 3). In particular, all the poles and zeros were in the left half of the plane, which is necessary for a stable system. The range of DC gain level for the group of rabbits was between 51 and 62 dB (58.5 ± 1.8 dB, means ± SE). The coherence between stimulus and the RBF response was >0.5 until ~0.9 Hz in every rabbit.

Estimation of model error. To calculate the error in the model, the transfer function calculated for each rabbit was used to simulate RBF from the recorded stimulus signal. To accommodate the pure time delay of 0.67 s, the data were resampled to 15 Hz (from 2 Hz)

Table 1. *Fitted model parameters and the cost function value for each of 6 rabbits*

Rabbit	K	ω_1, Hz	ω_2, Hz	ω_3, Hz	ω_4, Hz	ω_5, Hz	ζ	τ, s	J
1	346.6	0.012	0.012	0.006	0.007	0.192	0.769	0.660	125.0
2	640.9	0.066	0.066	0.009	0.043	0.519	0.782	0.616	387.7
3	1271.5	0.071	0.071	0.007	0.769	0.155	0.539	0.735	2301.9
4	1215.5	0.030	0.005	0.001	0.263	0.062	2.236	0.734	309.8
5	1087.8	0.090	0.090	0.011	0.378	0.289	0.869	0.670	3016.4
6	929.7	0.032	0.032	0.013	0.013	0.448	0.592	0.619	2578.6
Mean	915.3	0.050	0.046	0.008	0.246	0.277	0.964	0.672	1453.2
SE	146.7	0.012	0.014	0.002	0.122	0.072	0.259	0.022	536.6

For ease of interpretation the values of the ω parameters are shown in Hz not the radians/s that was used in calculation. K, DC gain; ζ, damping factor; τ, time delay; J, cost function value.

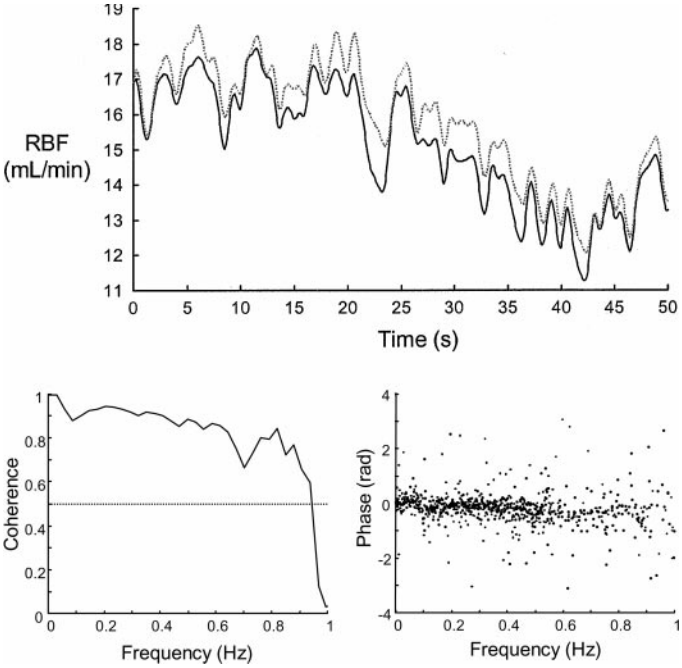

Fig. 4. *Top*: simulated RBF data (dotted line) compared with the measured RBF data (solid line) from a single rabbit. To allow the dynamics to be observed, 50 s of data from the 20-min period of PRBS stimulation has been shown with the mean of the simulated RBF data adjusted to equal that of the measured RBF data. *Bottom*: the coherence and phase difference calculated between the real and simulated data for 20 min of PRBS stimulation.

using a cubic spline interpolation technique. The resampled data were then used as the input to the transfer function. The output of the transfer function was subtracted from the steady-state value at the start of the stimulus to calculate the simulated RBF. The mean of the simulated RBF in every rabbit was lower than that of the recorded RBF. To allow the error in modeling the dynamics of the system to be calculated, only the data after 200 s of stimulation were used (to allow the RBF to reach a steady state) and the mean level of the simulated RBF was adjusted to equal that of the measured RBF. A typical 50 s of data for a single rabbit are shown in Fig. 4. The mean absolute percentage error (MAPE) was calculated using *Eq. 3*. The mean MAPE for the six rabbits was 5.7 ± 1.2%. *Equation 3* is the calculation of mean absolute percentage error between measured RBF and simulated RBF ($\hat{RBF}$), where n is the number of points.

$$\text{MAPE} = \frac{1}{n}\sum \frac{|\text{RBF} - \hat{\text{RBF}}|}{|\text{RBF}|} \times 100 \qquad (3)$$

Validation of PRBS. Previously we applied sinusoidal stimuli to the renal nerves and assessed the RBF response (11). Although the sinusoidal stimulus reveals only a limited amount of information as to the frequency response and would not allow one to determine a model structure, we felt it important to compare the two methods. Therefore in each of the six rabbits, sinusoidal stimulation at 0.04, 0.08, 0.12, 0.16, 0.2, 0.25, 0.32, 0.4, 0.5, and 0.72 Hz was applied for 7 min at each frequency (11). The gain and phase plots for a rabbit are shown in Fig. 5 and reveal that PRBS and sinusoidal stimulation gave qualitatively the same response.

DISCUSSION

In the present study we developed a mathematical model that describes the dynamic neural control over RBF. In particular we identified a complex system that cannot simply be described by a first-order model. Instead a more complex response composed of low-pass filter characteristics but with frequency ranges of constant gain was determined. Although our previous research had indicated a low-pass filtering characteristic of the vasculature (11), in the present study we precisely determined the nature of this response where SNA >0.2–0.3 Hz has a decreasing ability to be followed by the vasculature. In addition, we found two frequency ranges of interest, one extending from 0.001 to 0.006 Hz and the other from 0.01 to 0.2 Hz, where the gain in these ranges was constant or increased. The general shape of the frequency response was consistent across animals. We also found the time delay between the stimulus and the RBF responses to be very similar among animals, with an average of 672 ms. We propose that the identification of the precise relationship between SNA and RBF is a fundamental and necessary step toward understanding the interaction between SNA and other physiological mediators of RBF.

Previously the transfer function between arterial baroreceptors and blood pressure has been determined (7). Interestingly the gain and phase responses showed

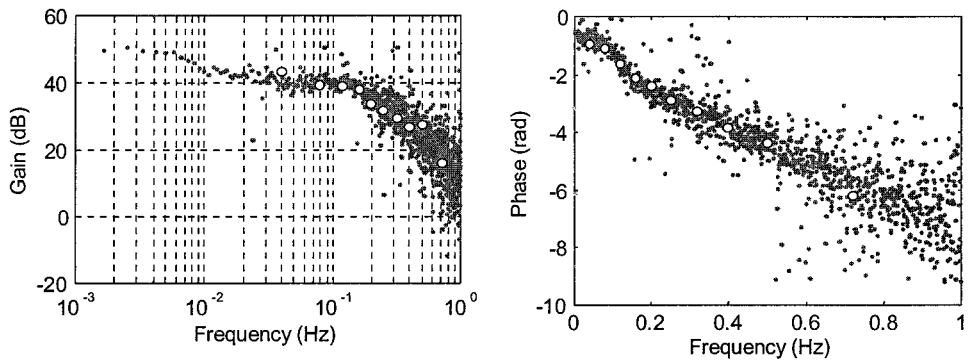

Fig. 5. Magnitude and phase data from a single rabbit response to PRBS stimulation (gray dots) and the sinusoidal stimulation (○).

similar trends to those calculated here. In particular the gain plots showed the expected low-pass filter characteristics, and the phase showed the linear relationship with frequency that suggests a pure time delay is present. Because the SNA to vasculature response is likely to comprise the largest component of the rate-limiting step in the overall baroreceptor control of the vasculature, it is possible that their (7) results reflect predominantly the frequency response of the vasculature to SNA.

We identified a pure time delay between the stimulus and the RBF response of 672 ms. The precise determination of this delay is an important step in understanding the origin of resonant oscillations within the cardiovascular system (2). In their study, Burgess et al. (3) used a differential-delay equation to model the baroreflex in the rat and reported that it predicts the 0.4-Hz rhythm present in blood pressure. Their model contained two time delays: one between efferent renal SNA and blood pressure fluctuations and a second time delay on the afferent side of the baroreflex. They estimated a time delay of 500 ms for the blood pressure response to SNA, which is not too dissimilar to that calculated from our model. The variation in the calculated pure time delay over the group of rabbits was small (672 ± 22 ms, means ± SD). Such little biological variation suggests that the contributors to this pure time delay comprised a series of time delays, e.g., neurotransmission and signal transduction whose properties are normally fixed.

In the past, attempts to model the frequency responses of the vasculature have been described using a structure of low-pass filters with a fixed time delay (1). In the present study we used the nomenclature of poles and zeros to describe the frequency response. Initially this may appear confusing; however, simply put, a pole indicates a frequency point at which the stimulus begins to exert less effect over RBF. The greater the number of poles, the less the vasculature will respond to the stimulus. A zero, on the other hand, indicates a frequency point at which the stimulus begins to exert more effect over RBF. Again, the greater the number zeros, the stronger the responsiveness of the vasculature. To some extent our model is simply a more complex low-pass filter with a time delay than previously presented (1). The advantage in using poles and zeros is that the parameters derived directly reflect the frequencies at which changes in gain occur.

The basis of the model developed is a 2 zero/4 pole system. Although the position of the poles and zeros varied among animals, this structure was present in each animal. At present, the physiological significance of either the structure of the model (2 zeros/4 poles) or the values of the parameters has not been determined. It is likely that the frequency positions of each of the poles and zeros are due to a physiological mediator. Examples could be vessel wall structure or intrinsic factors, such as nitric oxide or circulating angiotensin II. Our simulated model was able to describe 94% of the dynamic variation in RBF. The development of this model provides the basis for determining how a variety of mediators may interact with SNA over selective frequency ranges to modulate the RBF. For example, previously we found that blockade of endogenous nitric oxide dramatically increased the ability of RBF to oscillate in a resonant-like fashion to stimulation at 0.16 Hz (11).

One of the difficulties in assessing the impact of endogenous SNA on the renal vasculature is that a direct comparison among animals in the absolute microvolts levels is difficult due to the differences in contact between the recording electrode and the nerve between animals. Furthermore, determining a transfer function between the naturally occurring SNA signal and RBF is difficult for two reasons; first, the closed-loop nature of the system means that the effect of SNA on the RBF would feedback via blood pressure to alter subsequent SNA. Second, because SNA contains the majority of its power in select frequency bands (0.1–0.4 Hz, respiratory and cardiac) (9), the resulting transfer function may be valid only for those frequencies. Such an approach may miss important low-frequency interactions between SNA and the vasculature. The advantage of electrical stimulation is that it can produce a finely controlled input signal whose properties can be the same for all animals. However, the proviso remains that the mean level of voltage applied to the nerves cannot be related to the mean level of SNA and thus the mean RBF response, because electrical stimulation cannot mimic the selective recruitment of individual nerves that occurs with ongoing SNA and one cannot relate the mean voltage applied to the mean microvolts of ongoing SNA. However, the great advantage with PRBS stimulation is that it allows one to closely reflect the dynamic nature of ongoing SNA, and thus we propose that the RBF responses found in our study are indicative of the dynamic SNA control over the renal vasculature.

PRBS is a widely applied tool in engineering for determining the frequency response of systems and is a more convenient alternative to applying white noise as an input to physiological systems (8). Its advantage lies in the ability to stimulate with equal power at all frequencies of interest. Furthermore, in our experiment a frequency response could be determined in <30 min with a high-frequency resolution. Previous approaches to examining the frequency response have often applied single or trains of pulses at a variety of frequencies (13), for example, one pulse or train every 10 s to give a stimulus at 0.1 Hz. However, this approach means that the overall power applied to the nerve will diminish as the frequency reduces, making it difficult to compare between frequencies. Previously we investigated the frequency response by applying a sequence of sinusoidal amplitude-modulated stimulations at a number of frequencies (11). Although this approach applied the same power at all frequencies, the information provided was limited to 10 frequency steps that took up to 90 min.

Perspectives

Traditionally, analysis of cardiovascular control has been conducted using averages of the measured variables. Although such steady-state information can provide useful information on interactions among variables, it must be recognized that the cardiovascular system is dynamic, with much variability around the mean levels. In the case of SNA, the signal is well established to contain a number of frequencies: cardiac, respiratory, and slow (9). Although there has been intense clinical interest in quantifying slow oscillations in blood pressure and HR, with the hypothesis that these may reflect sympathetic drive, this clinical drive has been without a fundamental understanding of the origin of such variability. Clearly the way in which the various frequencies in SNA regulate blood flow is likely to be a major aspect in regulating blood pressure variability. In the present study, we investigated the dynamic neural regulation of the vasculature of the kidney. Using a stimulus and signal analysis tools, perhaps more at home in engineering, we have developed a mathematical model of the frequency response of the vasculature. Initially such modeling can seem esoteric and one is forced to answer the obvious question as to what physiological relevance model parameters, poles, and zeros may have? We propose that the model structure must be ultimately founded in a range of physiological mediators, such as the structural properties of the vasculature, circulating hormones, and intrinsic factors. Clearly the present study does not answer which of these is more important; however, the accurate determination of the frequency response with its constituent parameters provides the necessary framework to determine the physiological origin of a range of model parameters. With such knowledge, future experiments could be designed in which the system is perturbed, e.g., by altering the state of vasoconstriction within the vasculature and recording the changes in model parameters, rather as one does when considering changes in parameters derived from the sigmoidal baroreflex curve.

We conclude that the dynamic relationship between SNA and RBF is complex, comprising a low-pass filtering characteristic but also with frequency ranges of constant gain. We propose that the identification of the mathematical model for the relationship between SNA and RBF provides the framework for determining the dynamic interaction between SNA and other physiological mediators of RBF.

This work was funded by a grant from the Marsden Fund.

REFERENCES

1. **Betram D, Barres C, Cheng Y, and Julien C.** Norepinephrine reuptake, baroreflex dynamics, and arterial pressure variability in rats. *Am J Physiol Regulatory Integrative Comp Physiol* 279: R1257–R1267, 2000.
2. **Bertram D, Barres C, Cuisinaud G, and Julien C.** The arterial baroreceptor reflex of the rat exhibits positive feedback properties at the frequency of mayer waves. *J Physiol (Lond)* 513: 251–261, 1998.
3. **Burgess DE, Hundley JC, Li SG, Randall DC, and Brown DR.** First-order differential-delay equation for the baroreflex predicts the 0.4-hz blood pressure rhythm in rats. *Am J Physiol Regulatory Integrative Comp Physiol* 273: R1878–R1884, 1997.
4. **Holstein-Rathlou NH and Leyssac PP.** Oscillations in the proximal intratubular pressure: a mathematical model. *Am J Physiol Renal Fluid Electrolyte Physiol* 252: F560–F572, 1987.
5. **Holstein-Rathlou NH and Marsh DJ.** A dynamic model of renal blood flow autoregulation. *Bull Math Biol* 56: 411–429, 1994.
6. **Holstein-Rathlou NH and Marsh DJ.** Renal blood flow regulation and arterial pressure fluctuations: a case study in nonlinear dynamics. *Physiol Rev* 74: 637–681, 1994.
7. **Kawada T, Sato T, Shishido T, Inagaki M, Tatewaki T, Yanagiya Y, Sugimachi M, and Sunagawa K.** Summation of dynamic transfer characteristics of left and right carotid sinus baroreflexes in rabbits. *Am J Physiol Heart Circ Physiol* 277: H857–H865, 1999.
8. **Khoo MCK.** *Physiological Control Systems: Analysis, Simulation and Estimation*. New York: IEEE Press, 2000.
9. **Malpas SC.** The rhythmicity of sympathetic nerve activity. *Prog Neurobiol* 56: 65–96, 1998.
10. **Malpas SC and Evans RG.** Do different levels and patterns of sympathetic activation all provoke renal vasoconstriction? *J Auton Nerv Syst* 69: 72–82, 1998.
11. **Malpas SC, Hore TA, Navakatykyan M, Lukoshkova EV, Nguang SK, and Austin PC.** Resonance in the renal vasculature evoked by activation of the sympathetic nerves. *Am J Physiol Regulatory Integrative Comp Physiol* 276: R1311–R1319, 1999.
12. **Malpas SC and Leonard BL.** Neural regulation of renal blood flow: a re-examination. *Clin Exp Pharm Physiol* 27: 956–964, 2000.
13. **Stauss HM, Stegmann JU, Persson PB, and Habler HJ.** Frequency response characteristics of sympathetic transmission to skin vascular smooth muscles in rats. *Am J Physiol Regulatory Integrative Comp Physiol* 277: R591–R600, 1999.